Int. J. Heat Mass Transfer. Vol. 33, No. 4, pp. 691–701, 1990
Printed in Great Britain

0017–9310/90 $3.00 + 0.00

Modeling of confined turbulent fluid–particle flows using Eulerian and Lagrangian schemes

A. ADENIJI-FASHOLA and C. P. CHEN
Department of Mechanical Engineering, The University of Alabama in Huntsville, Huntsville, AL 35899, U.S.A.

(*Received* 9 *January* 1989 *and in final form* 20 *June* 1989)

Abstract—Two important aspects of fluid–particulate interaction in dilute gas–particle turbulent flows, namely the turbulent particle dispersion and the turbulence modulation effects, are addressed using the Eulerian and Lagrangian modeling approaches to describe the particulate phase. Gradient diffusion approximations are employed in the Eulerian formulation while a stochastic procedure is utilized to simulate turbulent dispersion in the Lagrangian formulation. The k–ε turbulence model is used to characterize the time and length scales of the continuous phase turbulence. Models proposed for both schemes are used to predict turbulent, fully-developed gas–solid vertical pipe flow with reasonable prediction accuracy.

INTRODUCTION

TWO-PHASE turbulent dispersed flows are encountered in a wide variety of engineering applications. Examples of such flows include the pneumatic transport of particulate materials, two-phase gasification and combustion and environmental pollution. Strong couplings between the continuous and dispersed phases are the main characteristics of these flows. Recently, mathematical models, which include numerical methods and physical models, capable of predicting particle velocity and concentration have become very important tools in understanding these two-phase flow processes. Turbulence also plays a dominant role in determining particle or droplet dynamics. Any realistic predictive model should thus be able to account for the turbulent dispersion of dispersed phases.

In general, two-phase flows are too complex to be treated in a complete way. Basically, there are two approaches commonly used to predict particulate two-phase flows. One, called the Lagrangian or 'tracking' approach, treats the particles as discrete entities in a turbulent flow field and their trajectories are calculated. The mutual coupling between fluid and particles is accounted for by estimating the particle source term for each computational cell visited by the particle. This is followed by a recalculation of the flow field incorporating these source terms. The other approach is the so-called 'two-fluid' model or Eulerian approach. In this approach, the cloud of particles is regarded as a continuum and the appropriate governing equations in differential form are solved for both phases. The effect of two-way coupling is incorporated as extra source terms in the continuum equations for both phases. The mechanism of including the turbulent dispersion effect is very different for each approach in view of the inherent difference in the two descriptions. The Lagrangian model employs the Monte Carlo procedure to calculate dispersed phase properties such as the number density distribution and the mean and fluctuating particle velocities. On the other hand, phenomenological models are required to close the time-averaged conservation equations for both phases in the Eulerian approach. Often, gradient type models are used to relate the turbulent particle flux to the mean particle concentration gradient to account for dispersion effects.

Both approaches have been studied extensively in the last decade and excellent reviews of recent developments in both modeling schemes exist [1–4]. Comparative performances of these two approaches have also been investigated very recently [5, 6]. At the present time, it is not universally accepted which approach is more valid for simulating particulate turbulent flows, since each appears to have inherent advantages and weaknesses. The aim of the present study is to compare the Lagrangian and Eulerian models with the simultaneous inclusion of two important aspects of the fluid–particle interactions—the turbulent particle dispersion (the influence of fluid turbulence on the particles), and the 'modulation' effects [7] (the influence of the particles on fluid flow turbulence). These two phenomena have often been neglected in most of the previous numerical modeling studies. Comparative studies between the two-fluid and tracking methods in which turbulence effects are included have also not been reported in the literature for wall-bounded flows. In particular, the inclusion of the modulation effect in the Lagrangian formulation for confined flows represents a novel contribution.

GOVERNING EQUATIONS

In this section, we present the assumptions made and the forms of the governing equations adopted for predicting turbulent, confined gaseous flows laden

NOMENCLATURE

A_p projection area of a particle ($\pi d_p^2/4$ for a spherical particle)
C_D drag coefficient
C_μ, C_1, C_2 turbulence model constant
D nozzle or pipe diameter
D_p, D_t turbulent eddy diffusivity
d_p particle diameter
F_{pi} interphasal interaction force
f_α fraction of particles belonging to diameter group α
f_β fraction of particles leaving starting location β
G particulate mass fluxes
G_k turbulence kinetic energy production
g gravity
k continuous phase turbulent kinetic energy
k_p particulate phase turbulent kinetic energy
l_e eddy size
$\dot{m}^p$ particle mass flow rate
$\dot{N}^p$ particle number flow rate
P, p pressure
Re flow Reynolds number
Re_p particle Reynolds number
Sc_p, Sc_t particle, turbulent Schmidt number
t_* particle relaxation time.

Greek symbols
γ numerical constant introduced in equation (23)
δ_{ij} Kronecker delta
ε dissipation rate of turbulent kinetic energy
θ volume fraction of particles
μ, ν molecular and kinematic viscosity of fluid
ν_t eddy viscosity of continuous phase
ν_p eddy viscosity of dispersed phase
ρ continuous phase density
ρ_p particulate phase loading, $\rho_s\theta$
ρ_s material density of the particle
τ Kolmogorov time scale.

with solid particles. The assumptions implied in the present study are as follows.

(1) The particulate phase is dilute and comprised of a monodisperse particle size distribution for which particle–particle interactions are negligible but fluid–particle two-way interaction is allowed.
(2) The fluid phase is Newtonian and possesses constant physical properties.
(3) The mean flow is steady, axisymmetric, incompressible and isothermal.
(4) Molecular diffusion and the Brownian motion effect on the particulate phase are negligible compared with turbulent dispersion.
(5) Triple correlations involving fluctuations in the particulate phase density are negligible.

The criteria, under which these assumptions as well as the continuum approach conditions are valid, have been discussed in ref. [8]. The derivations of the governing equations for the continuous phase in Eulerian form and for the dispersed phase in both the Eulerian and Lagrangian formulation are given by Soo [9], Hinze [10], Dukowicz [11], and Drew [12]. These equations are summarized in the following sections.

Continuous phase equations

Equations for the mean turbulent motion are obtained by applying the Reynolds decomposition and time averaging the instantaneous continuity and momentum equations

$$\frac{\partial}{\partial x_j}(\rho U_j) = 0 \tag{1}$$

$$\frac{\partial}{\partial x_j}(\rho U_i U_j) = -\frac{\partial}{\partial x_i}P + \frac{\partial^2}{\partial x_j \partial x_j}\mu U_i - \frac{\partial}{\partial x_j}(\overline{\rho u_i' u_j'}) + \bar{F}_{pi}. \tag{2}$$

Both Lagrangian and Eulerian approaches use equations (1) and (2) for the underlying continuous phase mean flow. However, the expression for $\bar{F}_{pi}$, which will be described later, differs for either approach.

Dispersed phase equations—Eulerian

In this approach the dispersed phase is treated as a continuum. The 'dusty gas' equations of Marble (as contained in refs. [8, 13]) form the governing equations for the dispersed phase. They are

$$\frac{\partial}{\partial x_j}(\bar{\rho}_p V_j) + \frac{\partial}{\partial x_j}(\overline{\rho_p' v_j'}) = 0 \tag{3}$$

$$\frac{\partial}{\partial x_j}(\bar{\rho}_p V_i V_j) = -\frac{\partial}{\partial x_j}(\bar{\rho}_p \overline{v_i' v_j'} + \overline{\rho_p' v_i'} V_j + \overline{\rho_p' v_j'} V_i) - \bar{F}_{pi}. \tag{4}$$

The previously mentioned assumptions exclude the triple correlation and pressure field in equation (4). The second-order correlations in equations (3) and (4) are the turbulent fluxes of momentum and turbulent dispersion of particles which require modeling.

Dispersed phase equations—Lagrangian

An alternative treatment of the dispersed phase involves the tracking of individual particles as they

move through the turbulence field of the continuous phase. This is essentially a statistical approach and requires the tracking of a sufficiently large number of individual particles in order to obtain statistically stationary information for the dispersed phase. This approach has been adopted by Dukowicz [11], Crowe *et al.* [14], Shahnam and Jurewicz [15], and Shuen *et al.* [16, 17] among others.

The usual starting point for the Lagrangian, particle tracking approach is the equation of motion of a particle within a fluid continuum which was originally derived by Basset, Boussinesq, and Oseen, hence the B–B–O equation (Soo [9]). For the particular case of the motion of solid spheres for which $\rho \ll \rho_s$, the approximate form of the B–B–O equation of motion, subject to the previously stated assumptions, is

$$\frac{dv_i}{dt} = \frac{(u_i - v_i)}{\tau_*} + g_i. \tag{5}$$

Equation (5) represents a form in which the virtual mass term, Basset term, and pressure gradient from the fluid acceleration term have been neglected from the full B–B–O equation. For the cases considered in this study ($d_p \leqslant 200\ \mu m$), the most important term in this equation is the hydrodynamic drag force. The gravity force term can be neglected because the particle's settling velocity (which is proportional to the particle relaxation time multiplied by the gravitational acceleration) is at least one order of magnitude smaller than the particle's mean axial velocity. Solution of equation (5) yields the trajectory of an individual particle. In the most general form of the Lagrangian formulation, the velocities in equation (5) are the instantaneous values comprising the mean and fluctuating components. For a polydisperse particle size distribution, the particle size as well as other particle parameters are specified in a stochastic manner at the start of each particle's motion.

The interphase interaction force

The drag force $\bar{F}_{pi}$ which appears in the governing equations set is expressed from those of the standard experimental drag curve of a solid sphere with a constant diameter in a steady motion. In the Eulerian approach, $\bar{F}_{pi}$ is the time averaged part of the interaction force F_{pi} which has the form

$$F_{pi} = \frac{3}{4} C_D (v_i - u_i)|v_i - u_i| \frac{\rho}{\rho_s} \frac{\rho_p}{d_p} \tag{6}$$

where the drag coefficient, C_D, is the same as that used by Durst *et al.* [18] and is given by

$$C_D = \frac{24}{Re_p}(1 + 0.15 Re_p^{0.687}) \quad \text{and} \quad Re_p = \frac{|u_i - v_i| d_p}{\nu}. \tag{7}$$

Thus

$$\bar{F}_{pi} = \frac{1}{t_*}(1 + 0.15\overline{Re}_p^{0.687})\bar{\rho}_p(V_i - U_i) + \frac{1}{t_*}(1 + 0.15\overline{Re}_p^{0.687})\overline{\rho'_p(v'_i - u'_i)} \tag{8}$$

with

$$\overline{Re}_p = \frac{|U_i - V_i| d_p}{\nu}$$

and the particle relaxation time

$$t_* = d_p^2 \rho_s / 18 \rho \nu. \tag{9}$$

In the Lagrangian formulation, the interaction between the continuous phase and the dispersed phase is treated using the particle-source-in cell method of Crowe *et al.* [14]. In general, this involves calculating the mass, momentum, and energy sources due to a particle for each computational cell visited by the particle as it traverses the fluid continuum. These additional sources due to the particles are then introduced into the continuous phase equations during the next super-iteration. A sufficiently smooth particle source distribution is obtained if the number of computational particles representing groups of particles making up the whole population is large enough.

For the present study, only the momentum source term due to the particles is considered since there is no mass or thermal energy exchange between the phases for the isothermal flow investigated. For this case, the first term on the right-hand side of equation (5) becomes

$$\frac{3}{4} C_D \frac{\rho}{\rho_s d_p} |u_i - v_i|(u_i - v_i).$$

According to the numerical solution procedure used in this study, the flow domain is subdivided into a finite number of cells forming an orthogonal grid. The particles are introduced at a finite number of starting locations with a finite number of particle sizes at each starting location. The transfer of momentum between the phases is due to the drag force. Following Durst *et al.* [18], the particle momentum source term for any arbitrary control volume for particles of a single size group α and starting location β is

$$F_{pi}^{\alpha,\beta} = \dot{N}_p^{\alpha,\beta} \rho \frac{A_p^\alpha}{2} \int_{t_{in}}^{t_{out}} C_D |u_i - v_i^{\alpha,\beta}|(u_i - v_i^{\alpha,\beta})\, dt \tag{10}$$

where t_{in} and t_{out} are the times when the particle enters and leaves the control volume, respectively, and $\dot{N}_p^{\alpha,\beta}$ is the number flow rate of spherical particles of size group α and starting location β such that

$$\dot{N}_p^{\alpha,\beta} = \frac{6\dot{m}_p}{\pi \rho_p^\alpha (d_p^\alpha)^3} f_\alpha f_\beta. \tag{11}$$

The total momentum source due to all the particles that traverse the control volume is finally obtained as a summation over all such particles

$$F_{pi}^{cell} = \sum_{\alpha.cell} \sum_{\beta.cell} F_{pi}^{\alpha,\beta}. \quad (12)$$

Because of the averaging process, higher order terms appear in the continuous phase equations as well as in the Eulerian dispersed equations requiring closure schemes. As mentioned in the introduction, for the Lagrangian formulation, the effect of the turbulence on the particle motion will be simulated here by a stochastic approach. These will be described in the next section.

TWO-PHASE TURBULENCE MODELS

The hierarchy of turbulence closure models for single-phase flows range from simple mixing-length type zero-equation models to second-order mean Reynolds stress models where transport equations are solved for each component of the turbulent flux vectors and tensors. Extending the single-phase turbulence models to account adequately for turbulence–particle interactions has also been attempted recently [13, 19, 20]. The present modeling approach is based on the two-equation k–ε turbulence model. The turbulent stresses of equation (2) are modeled using a gradient constitutive equation

$$\overline{u_i'u_j'} = -\nu_t\left[\frac{1}{2}\left(\frac{\partial U_i}{\partial x_j}+\frac{\partial U_j}{\partial x_i}\right)\right]+\frac{2}{3}k\delta_{ij} \quad (13)$$

where the eddy viscosity of the carrier phase is given by

$$\nu_t = C_\mu k^2/\varepsilon. \quad (14)$$

In the two-phase flow situation, the continuous and dispersed phases interact with each other at both the mean and fluctuational levels. At the fluctuational level, the particles experience dispersion due to the action of the turbulence field while the turbulence field itself experiences a modulation effect due to the particles.

Turbulence dispersion

In an Eulerian model, particle dispersion is often modeled as a Fickian diffusion process, requiring the use of some sort of particle eddy diffusivity. Higher order particle dispersion models have also been proposed by Shih and Lumley [21]. Here we adopt the gradient type diffusion model of Chen and Wood [8] for the dispersed phase turbulent fluxes and particle dispersion by assuming the following relations:

$$\overline{v_i'v_j'} = -\nu_p\frac{1}{2}\left(\frac{\partial V_i}{\partial x_j}+\frac{\partial V_j}{\partial x_i}\right)+\frac{2}{3}\delta_{ij}\left(-\frac{1}{2}\overline{v_i'v_i'}+\nu_p\frac{\partial V_i}{\partial x_i}\right) \quad (15)$$

$$\overline{\rho_p'u_j'} = -D_t\frac{\partial\bar{\rho}_p}{\partial x_i}, \quad \overline{\rho_p'v_i'} = -D_p\frac{\partial\bar{\rho}_p}{\partial x_i}. \quad (16)$$

The use of the Boussinesq assumption for the particulate phase requires the definition of an 'effective' turbulent kinematic eddy viscosity, ν_p, and turbulent diffusivities, D_t and D_p. These are determined from the characteristics of the underlying turbulent motion by

$$\frac{\nu_p}{\nu_t} = \frac{1}{1+t_*/\tau_s} \quad (17)$$

$$D_t = \frac{\nu_t}{Sc_t} \quad \text{and} \quad D_p = \frac{\nu_p}{Sc_p} \quad (18)$$

where τ_s is the time macroscale of the turbulence and is evaluated as $\tau_s = 0.125k/\varepsilon$. The choice of turbulent Schmidt number was set to be $Sc_t = Sc_p = 0.7$ following the testing of Chen and Wood [13] for axisymmetric flows.

To account for dispersion effects in a Lagrangian model, particles have to be tracked through a continuous succession of turbulent eddies superimposed upon the mean flow of the continuous phase. Theoretically, it requires knowledge of the full time history of the turbulent flow, obtained by direct simulation from solving unaveraged unsteady Navier–Stokes equations. Since this is not yet feasible for most flows of practical interest, the turbulence is simulated by means of a stochastic process, whereby mean values are determined by equations (1) and (2). The instantaneous velocities for the continuous and dispersed phases are given by

$$u_i = U_i+u_i' \quad (19)$$

and

$$v_i = V_i+v_i' \quad (20)$$

respectively. The turbulence information required to evaluate the fluctuational component of the fluid velocity is obtained from the kinetic energy field obtained from the most recent super-iteration on the fluid phase equations. The approach adopted follows after those outlined by Gosman and Ioannides [22] and Shuen *et al.* [16, 17]. It is assumed that the turbulence is isotropic and that the fluctuational component of the fluid velocity is given by a Gaussian distribution the standard deviation σ_{ii} of which is given by

$$\sigma_{ii} = (2k/3)^{1/2}. \quad (21)$$

The fluctuational component of the velocity at any required location is then obtained by randomly sampling the distribution. The actual turbulence field encountered in pipe flow (wall-bounded flows in general) is anisotropic, thus requiring a non-Gaussian distribution of the turbulence intensity. Hence, the above assumption of a Gaussian distribution represents a significant simplification.

It is known that the B–B–O equation can only be rigorously solved after a complete space–time representation of the turbulent fluid flow field has been obtained. However, an approximation to this requirement can be achieved if the particle relaxation time, t^*, is of the same order of magnitude as the integral time scale of the turbulence field or smaller. This is

indeed the case in the present study. The integral time scale distribution of the turbulent flow field can be viewed as being equivalent to a distribution of turbulent eddies with which a particle interacts along its trajectory. The interaction time between a given eddy and the particle is taken as the smaller of the eddy lifetime (the integral time scale) and the particle transit time within the eddy, obtained as outlined below.

If the characteristic size of an eddy is assumed to be its dissipation length scale, l_e, where

$$l_e = C_\mu^{3/4} k^{3/2}/\varepsilon \tag{22}$$

the eddy lifetime is then estimated as

$$t_e = \sqrt{(3/2)\gamma C_\mu k/\varepsilon}. \tag{23}$$

Kallio and Stock [6] have deduced, from experimental measurements, that γ assumes values between 0.15 and 2.00. Faeth and co-workers have used the definition

$$t_e = l_e/(2k/3)^{1/2} \tag{24}$$

which corresponds to a value of $\gamma = 1.825742$ in equation (23) above. Gosman and Ioannides [22] used $t_e = l_e/|u'|$ where u' is the randomly sampled velocity fluctuation value from the distribution.

An estimate for the transit time of a particle within an eddy is obtained from the solution of a linearized form of the equation of motion of the particle as

$$t_{tr} = -t_* \ln\left[1.0 - l_e/t_*|u_i - v_i|\right]. \tag{25}$$

Effects of dispersed phase on turbulence

The above discussion concerns the effect of turbulence on the particle dispersion. It is now well known that even relatively small amounts of dispersed solids will modulate the turbulence structure of the carrying gas flow [23–25]. The interaction between particles and the continuous phase yield extra dissipation terms in the modeled equations for k and ε when turbulence modulation is considered. For the Eulerian treatment, the modulation effects were reflected in the extra dissipation terms in the k and ε equations, which were derived by including the interphase interaction force terms in the continuous phase. The model used in this study is based on the two-phase turbulent free shear flows of Chen and Wood [8] and is summarized as

$$\frac{\partial}{\partial x_i}(U_i k) = \frac{\partial}{\partial x_i}\left(\frac{\nu_t}{\sigma_k}\frac{\partial k}{\partial x_i}\right) + G_k - \varepsilon - \frac{\overline{\rho_p' u_i'}}{\rho t_*}(1 + 0.15\overline{Re_p}^{0.687})(U_i - V_i) \quad \text{(TH1)} - \frac{2k}{t_*}\frac{\tilde{\rho}_p}{\rho}\left[1 - \exp\left(-0.5 t_* \varepsilon/k\right)\right] \quad \text{(TH2)} \tag{26}$$

$$\frac{\partial}{\partial x_i}(U_i \varepsilon) = \frac{\partial}{\partial x_i}\left(\frac{\nu_t}{\sigma_\varepsilon}\frac{\partial \varepsilon}{\partial x_i}\right) + \frac{\varepsilon}{k}(C_1 G_k - C_2 \varepsilon) - 2\frac{\tilde{\rho}_p}{\rho}\frac{\varepsilon}{t_*} \quad \text{(TH3)} \tag{27}$$

where G_k, the turbulence kinetic energy production, is given by

$$G_k = \nu_t\left[2\left\{\left(\frac{\partial U_i}{\partial x_i}\right)^2 + \left(\frac{\partial U_i}{\partial x_j} + \frac{\partial U_j}{\partial x_i}\right)^2\right\}\right]. \tag{28}$$

The terms (TH2) and (TH3) are 'extra dissipation' terms due to the particle slip velocity at the fluctuation level. The model is valid for the situation $\tau_e \geqslant t_* \gg \tau$, where $\tau = (\nu/\varepsilon)^{1/2}$ is the Kolmogorov time scale. The model constants used are those given in ref. [26].

The implementation of the turbulence modulation effect within a Lagrangian formulation has been relatively ignored until very recently. Although the contributions of Shuen *et al.* [16, 17] seem to point in the right direction, the scheme used in this study follows the simpler approach proposed by Mostafa and Mongia [5]. The instantaneous particle source properties are known from the stochastic formulation; thus, the extra dissipation terms derived following conventional procedures [10] and appearing in the k equation are exact and require no modeling. However, the numerical procedure for these terms, especially for confined flows, is not fully established. We thus model the turbulence correlation between the relative velocity and the continuous phase component. In particular, the turbulence kinetic energy modulation term used in the Lagrangian formulation is similar to that developed by Chen and Wood [13] and presented in equation (26). The particulate phase loading, ρ_p, appearing in the expression is calculated using the particulate phase void fraction, θ, obtained for each cell as

$$\theta = \frac{1}{V}\sum_{\text{cell}}\left(\frac{\dot{m}_p^{\alpha,\beta}}{\rho_s}\right)(t_{\text{out}} - t_{\text{in}}) \tag{29}$$

where V is the cell volume. Equation (29) is consistent with the dilute particulate phase assumption, $\theta \ll 1$.

NUMERICAL SCHEME AND BOUNDARY CONDITIONS

The governing equations for the continuous phase, turbulence models, and Eulerian dispersed phase are solved numerically using a variant of the finite-volume-based code developed in ref. [27] for two-phase applications.

The scheme adopted for the Lagrangian approach is similar to that suggested by Crowe *et al.* [14]. First, the 'clean' fluid flow field is obtained by solving the continuous phase governing equations. Next, particle trajectories are computed for a predetermined number

of representative particles such that a statistically stationary solution is obtained for the overall particle flow field. A minimum of 1500 computational particles were employed for that purpose in the present investigation. The particle trajectories are obtained by solving the non-linear ordinary differential equation of motion subject to the currently existing continuous fluid flow field and using the fourth-order Runge–Kutta algorithm. During the calculation of the particle trajectories, the sources of momentum, kinetic energy and its rate of dissipation, all due to the particle motion, are accumulated for each computational cell of the flow field. These sources are then used in the next global iteration of the continuous phase flow field until convergence is attained.

In the current investigation of axisymmetric vertical pipe flow, a uniform grid of 50 axial nodes by 23 transverse nodes was used. A variable time step option was developed for the Runge–Kutta integration of the particle equation of motion. The time step was evaluated for each computational cell traversed based on the cell dimensions and the estimated residence time of the particle within the cell. This scheme ensured that source terms were computed for each cell visited by the particle, thus ensuring a smooth distribution of each source type for the entire flow field. This condition was attained by constraining the particle to undergo a minimum of four integration steps within each cell. Further details on this and other aspects of the Lagrangian scheme are available in ref. [26]. However, it is pertinent to also point out that in the particle trajectory calculations, the fluid properties utilized are those interpolated using the four nearest neighbor-nodes regarding the particle's current location, resulting in second-order accuracy [28] when compared with the more common approach of assuming the fluid properties to be uniform over the current cell within which the particle is located.

Boundary conditions—continuous phase

At the inlet plane, the axial velocity of the continuous phase is specified using the measured profile whenever possible. Otherwise, uniform profiles are assumed and the radial component is set to zero. Turbulent kinetic energy is assumed to be a fraction (3%) of the inlet mean kinetic energy and 3% of the characteristic length is used to evaluate the inlet dissipation. The conventional wall functions are used but modified to take into account the effects of particles. Some details are given in ref. [27]. At the exit plane, the boundary condition $\partial(\ )/\partial x = 0$ was imposed for all variables, equivalent to presuming fully-developed flow. Mass continuity of the continuous phase and dispersed phase was separately checked and corrected iteratively; details are available in ref. [26].

Boundary conditions—dispersed phase

The streamwise and transverse velocity components of the dispersed phase were set equal to those of the continuous phase in all cases at the inlet plane. The dispersed phase loading ratio $\bar{\rho}_p/\rho$ was prescribed as a uniform profile. At the wall of the confined chamber or pipe, a slip condition was imposed on the streamwise velocity component and the transverse component was set to zero at the walls in the Eulerian treatment. A no-flux or impermeable boundary condition was specified for $\bar{\rho}_p$ by setting $\partial\bar{\rho}_p/\partial n = 0$. In the Lagrangian treatment of the particulate phase, the boundary conditions have to be specified for each particle. It is recognized that the particle trajectory calculation is essentially an initial-value problem. However, it is necessary to specify the particle behavior at the symmetry axis and the wall since the particle motion takes place within a bounded domain.

RESULTS AND DISCUSSION

The validity of any numerical code for the prediction of physical phenomena rests on its ability to correctly simulate the available experimental data. In the present investigation, the experimental data of Tsuji *et al.* [24] for the vertical upflow of an air–particulate system in a straight pipe have been used.

Figure 1 shows the radial profile of the slip in the axial velocity between the air and the particulate phase as well as the predictions using the Eulerian and Lagrangian schemes. The mean particle size and the loading ratio are 200 μm and 1.0, respectively. It can be seen from the figure that both schemes predict the air velocity fairly accurately with the Eulerian scheme (ES) showing some underprediction in the 30% portion of the pipe near the wall. The Lagrangian scheme (LS), on the other hand, overpredicts the air velocity for the whole pipe except in the near-wall region. Both schemes yield better predictions of the particulate phase velocity. The crossover in the sign of the slip between the phases which occurs at about $0.20R$ from the wall is particularly well predicted by the Eulerian scheme. The crossover predicted by the Lagrangian scheme is at a location about $0.10R$ from the wall. The Lagrangian scheme shows a very good prediction of the particulate phase axial velocity in the central two-thirds of the pipe. However, there is considerable waviness in the particulate phase velocity profile which probably indicates that the 1500 computational particles (cps) used in the simulation are insufficient to obtain a smooth profile, even for the uniformly distributed particle concentration and mono-disperse size distribution used in the present study. This is in contrast to the findings of the study by Durst *et al.* [18] in which they report that 140 cps (or 10 cps per grid node) are sufficient to obtain smooth profiles. It should be noted, however, that the study by Durst *et al.* neglects both the effects of particle dispersion and turbulence field modulation.

In Fig. 2, we present results similar to those of Fig. 1 but for the higher particle loading ratio of 2.1. Here, the Eulerian scheme overpredicts the air velocity for most of the pipe except close to the wall. The Lagran-

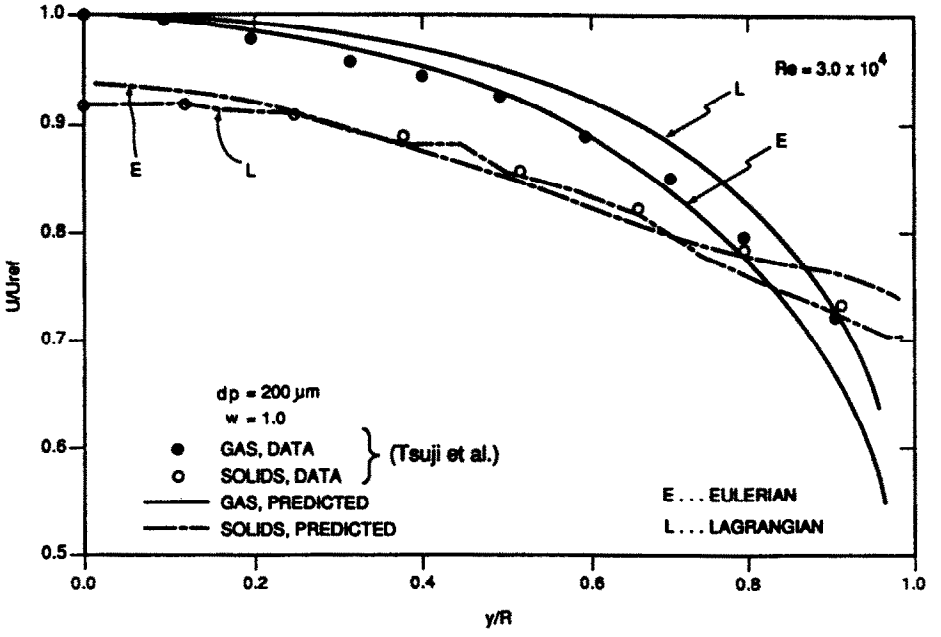

FIG. 1. Radial profiles of axial velocity in fully-developed vertical pipe upflow for solids loading ratio of 1.0.

gian scheme, on the other hand, yields a good prediction of the experimental results. With regard to the particulate phase velocity, ES produces an essentially flat profile across the pipe, underpredicting the data in the central half and overpredicting in the near wall region. LS, on the other hand, produces the proper trend but with some underprediction away from the central core.

The effect of the particulate phase on the axial air velocity profile as predicted by ES for particle loading ratios of 1.9 and 3.2 are presented in Fig. 3. The predictions are generally very good except for some

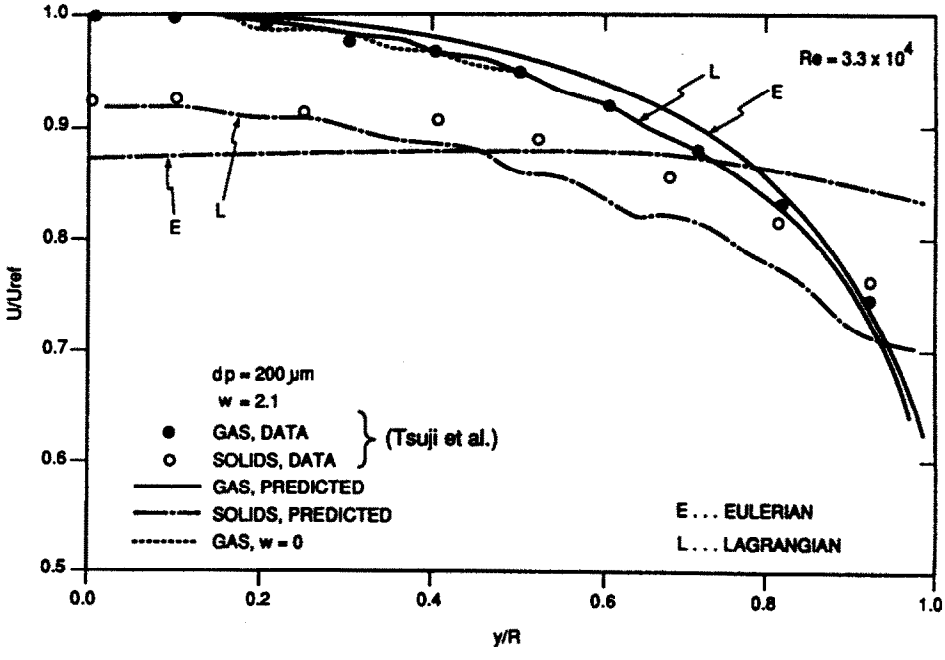

FIG. 2. Radial profiles of axial velocity in fully-developed vertical pipe upflow for solids loading ratio of 2.1.

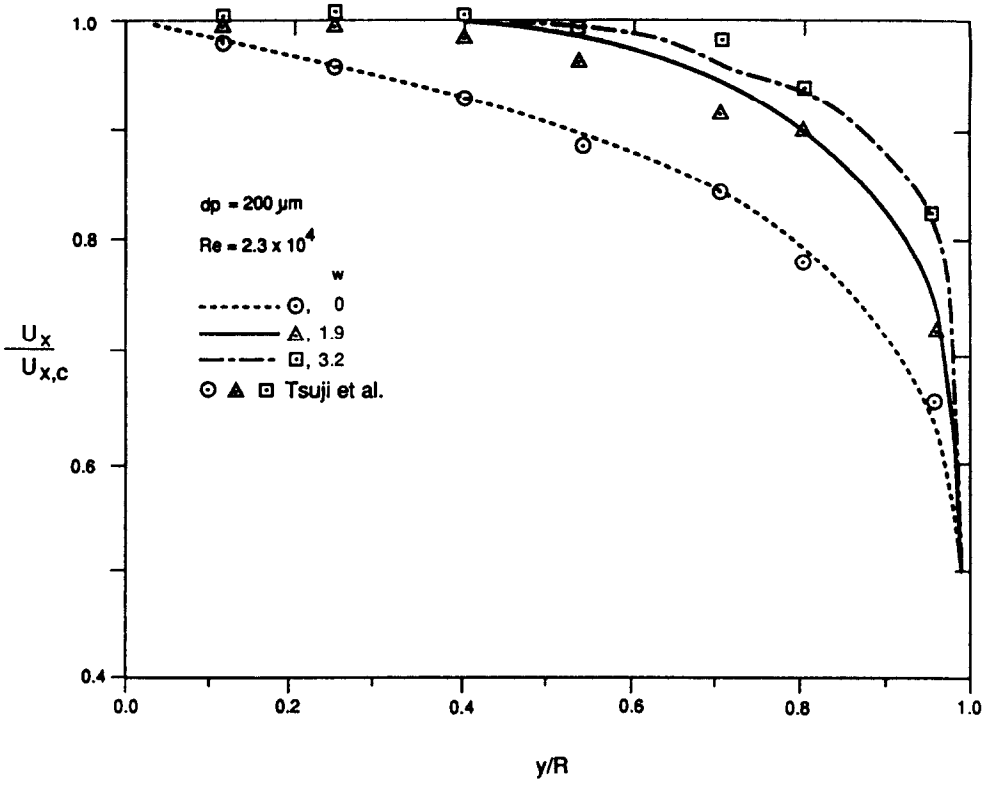

FIG. 3. Effect of particle loading on mean axial velocity profiles.

overprediction in the central two-thirds of the pipe for the 1.9 loading ratio case.

The turbulence modulation effects predicted by the two schemes for a loading ratio of 3.2 are shown in Fig. 4. The predictions are higher than the experimental values in every case shown except that by the Eulerian scheme in the central half of the pipe and for the loading ratio of 3.2. The experimental data exhibit increased modulation as we move away from the pipe axis and towards the wall. The LS predicts an opposite trend to this in which the maximum modulation is near the pipe axis. The ES, on the other hand, yields a constant modulation level across the pipe. It should be noted, however, that the modulation effect in such flows is a real one and needs to be included in prediction schemes in order to obtain more realistic results. Efforts to investigate the causes of the various trends observed in the modulation of the turbulence intensity depicted in Fig. 4 are continuing.

Figures 5 and 6 show the prediction of the normalized particle mass flux. In Fig. 5, which is a Lagrangian simulation, 1500 computational particles have been used while in Fig. 6, 9000 computational particles were used for the same experimental data. A mass flux value near the centerline of the inlet plane was used as the reference. The smoother profiles obtained with the 9000-particle simulation are obvious. Also included in Fig. 6 is the prediction obtained using the ES. The Eulerian scheme gave a uniform particle distribution at each cross-sectional plane of the pipe. However, the Lagrangian scheme yields a particle aggregation in the central portion of the pipe by the time the outlet plane is reached. This aggregation was not observed for the same experimental data when the Lagrangian scheme was run for a non-stochastic setting.

The computations for the current study were carried out on a Perkin–Elmer 3250 minicomputer. A typical ES run took about 1 h while a typical LS run required seven super iterations on the particle trajectory calculations using an under-relaxation factor of 0.5 for all source term computations and required about 4¼ h of CPU time. The required CPU time increased slightly with particle loading ratio giving an increase in CPU time of 1.6% between the lowest and the highest particle loading ratios computed.

CONCLUDING REMARKS

In summary, it has been demonstrated that the Eulerian scheme is less expensive to implement and gives better prediction of confined, turbulent fluid–particulate flows for the case of solid particles of about 200 μm diameter or less and for which $\rho_s/\rho \ll 1$ and $\theta_p \ll 1$. However, for fluid particulate phases in which

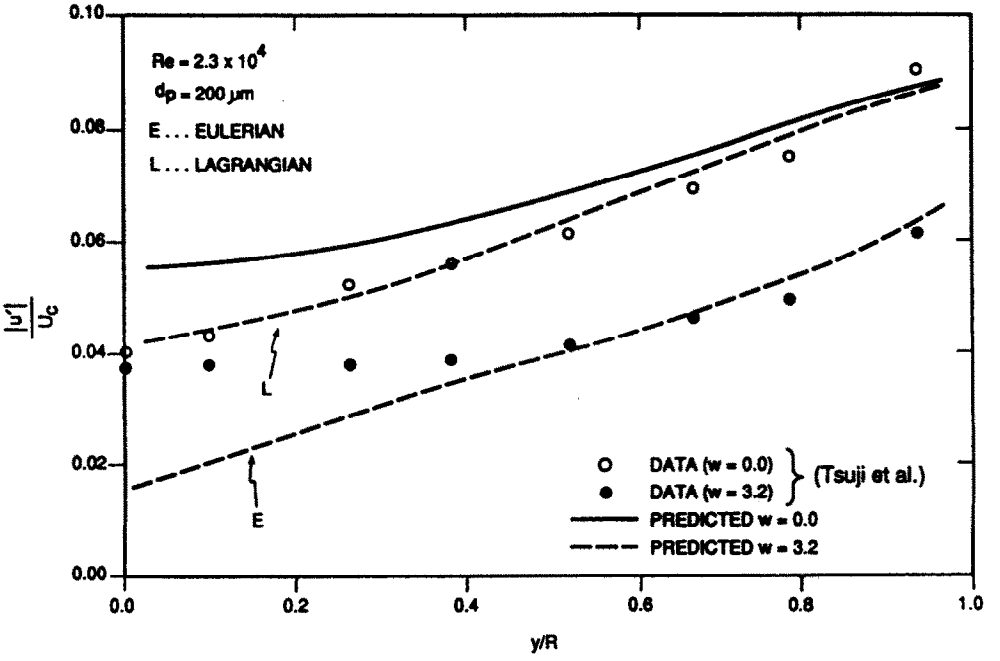

FIG. 4. Modulation effect of particles on the turbulence in the continuous phase for solids loading ratio of 3.2.

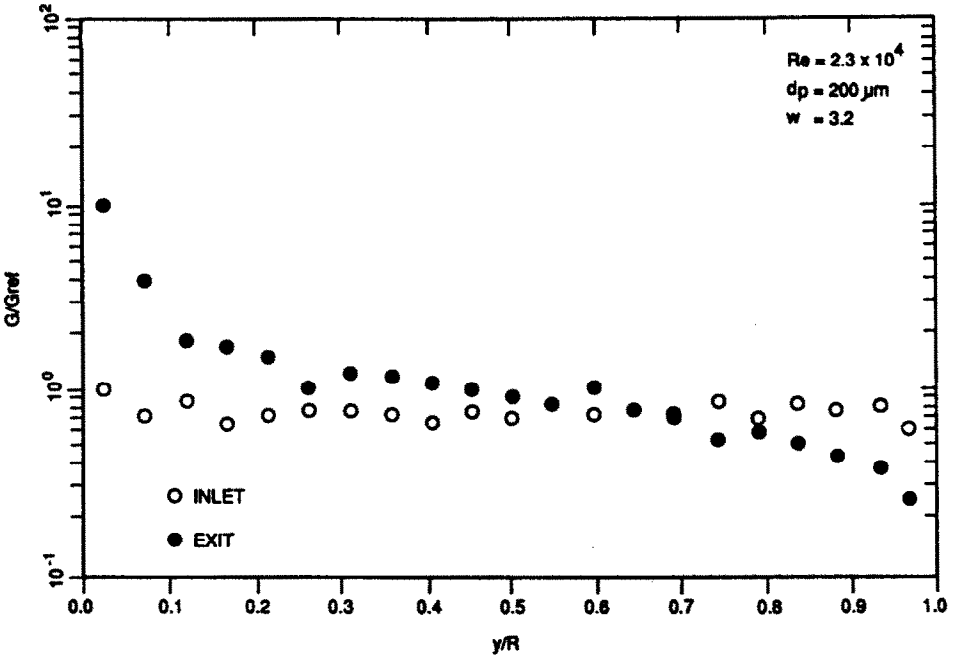

FIG. 5. Radial profile of particle mass flux for solids loading ratio of 3.2; 1500 computational particles used.

particle sizes change along particle trajectories so that a mono-disperse particle size assumption is unrealistic, the Lagrangian scheme is probably the only option.

The non-uniform particle concentration profile predicted using the LS still needs to be improved. This, we believe, is strongly dependent on the boundary condition specification for the particle trajectory calculation at the pipe axis. However, the predictions obtained in the present investigation for confined

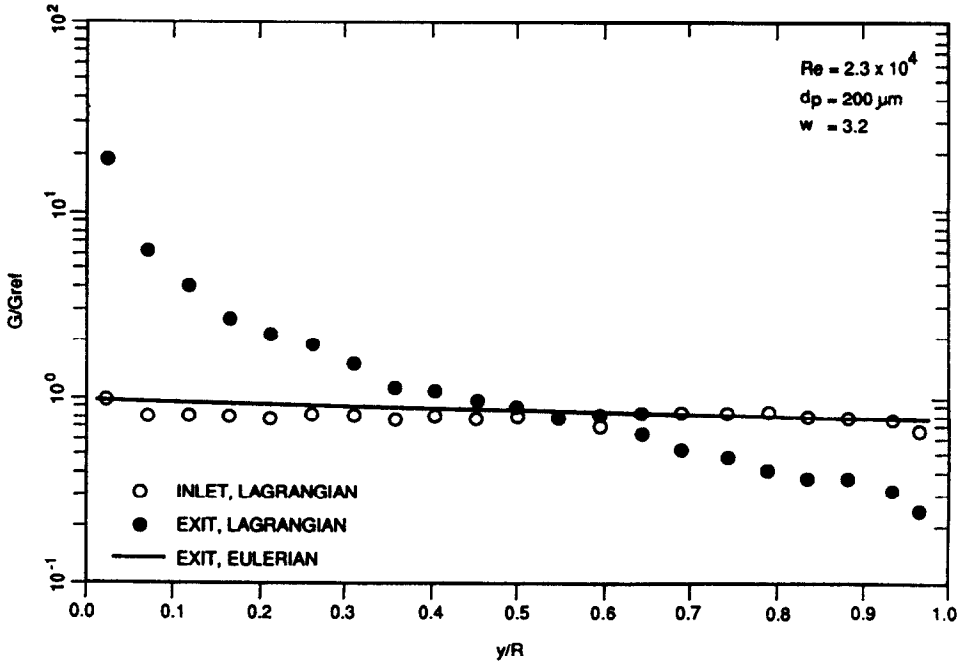

FIG. 6. Radial profile of particle mass flux for solids loading ratio of 3.2; 9000 computational particles used.

flows using the Lagrangian scheme in which the effect of both particle dispersion and turbulence field modulation have been incorporated represent a significant step forward in the use of the Lagrangian scheme for predicting turbulent fluid–particulate flows.

Acknowledgements—This work was carried out while the first author held a NASA–NRC Research Associateship at the NASA–George C. Marshall Space Flight Center. Financial support by NRC and NASA–MSFC is acknowledged.

REFERENCES

1. C. T. Crowe, Review—numerical methods for dilute gas–particle flows, *J. Fluids Engng* **104**, 297–303 (1982).
2. C. T. Crowe, Two-fluid versus trajectory model: range of applicability. In *Gas–Solid Flows*, ASME FED-Vol. 35, pp. 91–96 (1986).
3. J. L. Lumley, Two-phase and non-Newtonian flows. In *Turbulence* (Edited by P. Bradshaw), Chap. 7. Springer, Berlin (1978).
4. G. M. Faeth, Recent advances in modeling particle transport properties and dispersion in turbulent flow, *Proc. ASME–JSME Therm. Engng Conf.*, Vol. 2, pp. 517–534. ASME (1983).
5. A. A. Mostafa and H. C. Mongia, Eulerian and Lagrangian predictions of turbulent evaporating sprays, AIAA Paper 86-0452 (1986).
6. G. A. Kallio and D. E. Stock, Turbulent particle dispersion: a comparison between Lagrangian and Eulerian model approaches. In *Gas–Solid Flows*, ASME FED-Vol. 35, pp. 23–34 (1986).
7. A. M. Al-Taweel and J. Landau, Turbulence modulation in two-phase jets, *Int. J. Multiphase Flows* **3**, 341–351 (1977).
8. C. P. Chen and P. E. Wood, A turbulence closure model for dilute gas particle flows, *Can. J. Chem. Engng* **63**, 349–360 (1985).
9. S. L. Soo, *Fluid Dynamics of Multiphase Systems*, Chap. 2. Blaisdell, Waltham, Massachusetts (1967).
10. J. O. Hinze, Turbulent fluid and particle interaction, *Prog. Heat Mass Transfer* **6**, 433–452 (1972).
11. J. K. Dukowicz, A particle–fluid numerical model for liquid sprays, *J. Comp. Phys.* **35**, 229–253 (1980).
12. D. A. Drew, Mathematical modeling of two-phase flows, *Ann. Rev. Fluid Mech.* **15**, 261–291 (1983).
13. C. P. Chen and P. E. Wood, Turbulence closure modeling of the dilute gas–particle axisymmetric jet, *A.I.Ch.E. Jl* **32**, 163–166 (1986).
14. C. T. Crowe, M. P. Sharma and D. E. Stock, The particle-source-in cell (PSI-cell) model for gas–droplet flows, *J. Fluid Engng* **99**, 325–332 (1977).
15. M. Shahnam and J. T. Jurewicz, Particle motion near the inlet of a sampling probe. In *Gas–Solid Flows*, ASME FED-Vol. 35, pp. 145–153 (1986).
16. J.-S. Shuen, A. S. P. Solomon, Q.-F. Zhang and G. M. Faeth, A theoretical and experimental study of turbulent particle-laden jets, NASA CR 168293 (1983).
17. J.-S. Shuen, A. S. P. Soloman, Q.-F. Zhang and G. M. Faeth, Structure of particle-laden jets: measurements and predictions, *AIAA J.* **23**, 396–404 (1985).
18. F. Durst, D. Milojevic and B. Schonung, Eulerian and Lagrangian predictions of particulate two-phase flows: a numerical study, *Appl. Math. Model.* **8**, 101–115 (1984).
19. S. E. Elghobashi and T. W. Abou-Arab, A two-equation turbulence model for two-phase flows, *Physics Fluids* **26**, 931–938 (1983).
20. F. Pourahmadi and J. A. C. Humphrey, Modeling solid–fluid turbulent flows with application to predicting erosive wear, *Physicochem. Hydrodyn.* **4**, 191–219 (1983).
21. T. S. Shih and J. L. Lumley, Second order modeling of particle dispersion in a turbulent flow, *J. Fluid Mech.* **163**, 349–363 (1986).
22. A. D. Gosman and E. Ioannides, Aspects of computer simulation of liquid fueled combustors, AIAA Paper 81-0323 (1981).

23. D. Modarress, H. Tan and S. Elghobashi, Two-component LDA measurement in a two-phase turbulent jet, *AIAA J.* **22**, 624–630 (1984).
24. Y. Tsuji, Y. Morikawa and H. Shiomi, LDV measurements of an air–solid two-phase flow in a vertical pipe, *J. Fluid Mech.* **139**, 417–434 (1984).
25. S. L. Lee and F. Durst, On the motion of particles in turbulent duct flows, *Int. J. Multiphase Flow* **8**, 125–146 (1982).
26. A. A. Adeniji-Fashola, C. P. Chen and C. F. Schafer, Numerical predictions of two-phase gas–particle flows using Eulerian and Lagrangian schemes, NASA Technical Paper (1988).
27. C. P. Chen, Numerical analysis of confined recirculating gas–solid turbulent flows. In *Gas–Solid Flows*, ASME FED-Vol. 35, pp. 117–124 (1986).
28. W. A. Sirignano, Fuel droplet vaporization and spray combustion theory, *Prog. Energy Combust. Sci.* **9**, 291–322 (1983).

MODELISATION DES ECOULEMENTS TURBULENTS FLUIDE–PARTICULES PAR DES SCHEMAS EURELIENS ET LAGRANGIENS

Résumé—Deux aspects importants de l'interaction fluide–particules dans des écoulements turbulents, nomément la dispersion turbulente des particules et les effets de modulation de la turbulence, sont traités par la modélisation selon Euler et Lagrange pour décrire la phase particulaire. Des approximations du gradient de diffusion sont employées dans la formulation eulerienne tandis qu'une procédure stochastique est utilisée pour simuler la dispersion turbulente dans la formulation lagrangienne. Le modèle de turbulence k–ε est utilisé pour caractériser les échelles de temps et de longueur de la turbulence de phase continue. Les modèles proposés pour les deux schémas sont utilisés pour prédire l'écoulement gaz–solide turbulent pleinement établi dans un tube vertical avec une précision raisonnable.

MODELLIERUNG EINER BEGRENZTEN PARTIKELBELADENEN TURBULENTEN FLUIDSTRÖMUNG MIT HILFE DER BETRACHTUNGSWEISE NACH EULER UND LAGRANGE

Zusammenfassung—Zwei wichtige Seiten der Wechselwirkung in einer partikelbeladenen turbulenten Strömung von dünnem Gas, nämlich die Einflüsse der turbulenten Dispersion der Partikel und der turbulenten Modulation, werden mit Hilfe der Eulerschen und der Lagrangeschen Betrachtungsweise beschrieben. Im Fall der Eulerschen Betrachtung erfolgt die Näherung mittels gradientenbedingter Diffusion, während zur Simulation der turbulenten Dispersion ein stochastisches Verfahren in der Lagrangeschen Formulierung verwendet wird. Das k–ε-Turbulenzmodell wird benutzt, um das Zeit- und Längenmaß der Turbulenz der kontinuierlichen Phase zu charakterisieren. Die für beide Verfahren vorgeschlagenen Modelle werden angewandt, um die voll ausgebildete turbulente Gas/Feststoffströmung in einem senkrechten Rohr mit einer angemessenen Genauigkeit zu berechnen.

МОДЕЛИРОВАНИЕ ОГРАНИЧЕННЫХ ТУРБУЛЕНТНЫХ ПОТОКОВ ЖИДКОСТИ И ЧАСТИЦ С ИСПОЛЬЗОВАНИЕМ СХЕМ ЭЙЛЕРА И ЛАГРАНЖА

Аннотация—Используя Эйлеров и Лагранжев подходы для описания отдельных фаз в разбавленных турбулентных потоках газа с частицами, исследованы два важных аспекта межфазного взаимодействия, а именно, турбулентная дисперсия частиц и эффекты модуляции турбулентности. В формулировке Эйлера используются приближения градиентной диффузии, в то время как в формулировке Лагранжа для моделирования турбулентной дисперсии используется стохастический метод. Для характеристики масштабов времени и длины турбулентности газовой фазы применяется k–ε модель. Предложенные в обеих схемах модели используются для достаточно точного расчета турбулентного полностью развитого течения газа и частиц в вертикальной трубе.